

## The crystal structure of namuwite, a mineral with Zn in tetrahedral and octahedral coordination, and its relationship to the synthetic basic zinc sulfates

LEE A. GROAT

Department of Geological Sciences, University of British Columbia, Vancouver, British Columbia V6T 1Z4, Canada

### ABSTRACT

The crystal structure of namuwite,  $(\text{Zn,Cu})_4\text{SO}_4(\text{OH})_6 \cdot 4\text{H}_2\text{O}$ , trigonal,  $a = 8.331(6)$ ,  $c = 10.54(1)$  Å,  $V = 634(1)$  Å<sup>3</sup>,  $P\bar{3}$ ,  $Z = 2$ , has been solved by direct methods and refined to an  $R$  index of 7.9% using  $\text{MoK}\alpha$  X-ray data. The fundamental building unit of the structure is a gently modulated sheet of edge-sharing (Zn,Cu) octahedra parallel to (001), with one vacancy for every six occupied octahedral sites. The sheets are decorated on both sides by  $\text{SO}_4$  and  $[\text{Zn}(\text{OH})_3(\text{H}_2\text{O})]^{1-}$  tetrahedra; the latter are located above and below the vacant octahedral sites. Adjacent tetrahedral-octahedral-tetrahedral (T-O-T) layers are held together by hydrogen bonds to interstitial  $\text{H}_2\text{O}$  molecules.

In synthetic  $\text{Zn}_4\text{SO}_4(\text{OH})_6 \cdot 4\text{H}_2\text{O}$  successive octahedral layers are displaced by  $\frac{1}{2}[a + b]$ . In namuwite, this is not the case, which suggests that the presence of Cu in the octahedral sites prevents this from happening. Namuwite undergoes a reversible transition, probably to the pentahydrate phase, at approximately room temperature.

### INTRODUCTION

Namuwite,  $(\text{Zn,Cu})_4\text{SO}_4(\text{OH})_6 \cdot 4\text{H}_2\text{O}$ , was first described by Bevins et al. (1982) from the Aberllyn lead mine in Wales, where it occurs with hydrozincite on a breccia composed of slate fragments cemented by sphalerite, quartz, calcite, and ankerite. Namuwite has also been described from the Dyfnwgwm, Dylife, and Smallcleugh mines in Wales (Livingstone et al. 1990); from Vincenza, Italy (Bertoldi et al. 1984); Laurion, Greece (Rewitzer and Hochleitner 1989); Tsumeb, Namibia (Schnorrer-Köhler 1986); and from several localities in Germany (Schnorrer-Köhler et al. 1988). The material studied by Bevins et al. (1982) occurred as aggregates of perfect to subperfect hexagonal plates up to 60  $\mu\text{m}$  across. Their indexing of powder X-ray diffraction data was performed on the basis of a hexagonal cell with  $a = 8.29$  and  $c = 10.50$  Å. Systematic absences suggested that possible space groups are  $P6$ ,  $P\bar{6}$ ,  $P6/m$ ,  $P622$ ,  $P6mm$ ,  $P\bar{6}m2$ ,  $P\bar{6}2m$ , and  $P6/mmm$  (Bevins et al. 1982).

The samples used in this study are from Granetal in the Harz Mountains, Germany. They occur with two habits: as tabular crystals with a hexagonal outline and as needlelike crystals with a trigonal outline and perfect cleavage perpendicular to the needle axis. The crystals were previously studied by the late Renate von Hodenberg, who found evidence of a phase transition between 0 and 45 °C, in which the  $c$  dimension increased from 10.4 to 10.9 Å (W. Krause, personal communication).

This work is part of a long-term study of the copper oxysalt minerals. Namuwite is of particular interest because it is hydrated, and our understanding of hydrated structures has generally progressed at a slower rate than our understanding of anhydrous compounds, as is evi-

dent from the compendium of copper oxysalt structures presented by Eby and Hawthorne (1993).

### CHEMICAL ANALYSES

Electron microprobe analyses were conducted with a Cameca SX-50 instrument equipped with one energy-dispersion (ED) spectrometer and four automated wavelength-dispersion (WD) spectrometers. ED spectra showed no elements other than Zn, Cu, S, and O. All WD analyses were conducted with an accelerating potential of 15 kV and a sample current of 10 nA. Counts for each element were collected for 20 s. The beam was intentionally defocused to a diameter of 25  $\mu\text{m}$  to minimize damage to the sample. Back-scattered electron (BSE) imaging showed no compositional zoning or intergrowths. The standards used were sphalerite (Zn, S) and covellite (Cu). Data reduction was achieved using conventional ZAF techniques. The analyses, shown in Table 1, are normalized on the basis of five cations per formula unit. The high totals associated with the analyses of this study are due to the loss of  $\text{H}_2\text{O}$  through volatilization during data collection. The low totals of the analyses from Livingstone et al. (1990) suggest that one of the cations is underdetermined; by comparison with the other analyses, this is probably Zn. The analysis of Bevins et al. (1982) used atomic absorption spectrometry (AAS, for Zn and Cu) and thermogravimetric analysis (TGA, for S and  $\text{H}_2\text{O}$ ).

Analyses of the crystals used in this study show approximately 20 at% Cu in the Zn sites. This is appreciably less than the 37% reported by Bevins et al. (1982) and the 43% given by Livingstone et al. (1990), which are

TABLE 1. Chemical composition of namuwite

	This study*	Livingstone et al. (1990)**	Bevins et al. (1982)†
ZnO	53.02	32.28	37.8
CuO	13.16	23.48	22.0
SO <sub>3</sub>	14.04	13.73	14.9
H <sub>2</sub> O	25.03‡	21.77‡	24.5
Total	105.25	91.26	99.2
Zn	3.28	2.30	2.51
Cu	0.83	1.71	1.49
S	0.88	0.99	1.00
O	13.77	13.99	14.34

Note: Oxides are in weight percent; analyses are normalized on five cations per formula unit.

\* Average of five electron microprobe analyses.

\*\* Average of three electron microprobe analyses.

† Zn and Cu by AAS; SO<sub>3</sub> and H<sub>2</sub>O by TGA.

‡ Calculated by stoichiometry, assuming four H<sub>2</sub>O molecules per formula unit.

both higher than the maximum of 33% reported by Gilbert (1977) for synthetic (Zn,Cu)<sub>4</sub>SO<sub>4</sub>(OH)<sub>6</sub>·4H<sub>2</sub>O.

### STRUCTURE DETERMINATION

Numerous crystals of both tabular and needlelike morphologies were mounted on a Nicolet R3m automated four-circle diffractometer equipped with a molybdenum-target X-ray tube (operating at 55 kV, 40 mA) and a graphite crystal monochromator mounted with equatorial geometry. Random orientation photographs of the crystals showed faint rings (similar to those seen in photographs of microcrystalline aggregates) and a small number of broad, very diffuse spots. In most cases the diffractometer was unable to center on these reflections. However, random orientation photographs of one tabular crystal showed reflections that appeared less diffuse than those of the others, and the centers of nine of these reflections were determined. Least-squares refinement of these reflections produced hexagonally constrained cell dimensions,  $a = 8.331(6)$  and  $c = 10.54(1)$  Å.

Intensity data were collected in the  $\theta$ - $2\theta$  scan mode, using 96 steps with a scan range from  $[2\theta(\text{MoK}\alpha_1) - 1.1]$  to  $[2\theta(\text{MoK}\alpha_2) + 1.1]^\circ$  and a variable scan rate between 3.91 and 29.3°/min depending on the intensity of an initial one-second count at the center of the scan range. Backgrounds were measured for one-half the scan time at the beginning and end of each scan. Two standard reflections were monitored every 46 measurements to check for stability and constancy of crystal alignment. Eventually, it was discovered that the intensities of reflections collected overnight were much lower than those collected during the day. The count rate (Fig. 1) would begin falling every day at approximately 23:00, reaching minimum levels of approximately zero counts per second about 6 h later. By 07:00, all intensities had returned to their normal daytime levels.

It was obvious that the crystal was undergoing a reversible transition. Random orientation photographs taken in the middle of the night showed diffuse rings and

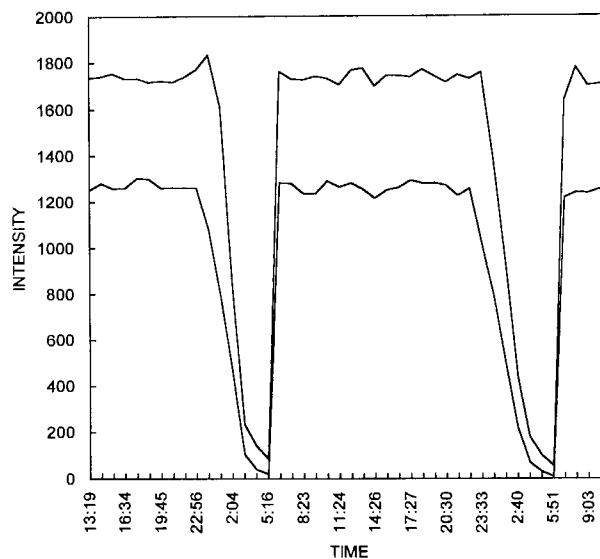


FIGURE 1. Time (hours:minutes) vs. intensity (counts per second) for check reflections 131 (top) and 320 (bottom), from the first namuwite data collection.

a few very weak spots. The diffractometer was unable to center on any of these reflections.

Further investigation revealed that every room in the (new) building had a heat source controlled by a central computer. To save energy, these were turned off every day at 20:00. By 05:00, when the heat sources were turned on again, the room temperature was at a minimum, and it would take about 2 h for the room to warm up to the normal daytime temperature of approximately 24 °C. Reflection intensities would begin falling at about 23:00, when the room temperature was approximately 22 °C, and reach a minimum at about 05:00, when the room was coldest. Presumably, the building would heat up rapidly once the heat sources were turned on, which would account for the return to normal intensity levels by 07:00.

After completion of the first data collection, a second data collection was initiated at a different time of day to obtain reflections missing from the original data set. The final merged dataset comprised 2065 reflections representing two asymmetric units from 3–60°  $2\theta$ . Scale factors were refined independently for data from each collection. Absorption corrections had no effect on the  $R$  (merging) index (presumably because the reflections were so weak) and were not used. After correction for Lorentz, polarization, and background effects, the data were averaged and reduced to structure factors. The  $R$  index for the averaging procedure was 8.1%. Of the 1242 unique reflections, 493 were classed as observed, i.e., with magnitudes greater than six standard deviations on the basis of counting statistics. Miscellaneous information pertaining to data collection is given in Table 2.

The Siemens SHELXTL PC system of programs was used throughout this work. Scattering curves for neutral atoms together with anomalous dispersion coefficients

TABLE 2. Miscellaneous information for namuwite

$a$ (Å)	8.330(1)	Radiation; mono	MoK $\alpha$ ; graphite
$c$ (Å)	10.540(2)	Unique intensities	1242
$V$ (Å <sup>3</sup> )	634(1)	No. of $ F_o  > 6\sigma$	485
Space group	$P\bar{3}$	$R_{obs}$ (%)	7.9
Crystal size (mm)	0.08 × 0.08 × 0.11	$R_{w,obs}$ (%)	9.3
Cell content	2[(Zn,Cu) <sub>2</sub> SO <sub>4</sub> (OH) <sub>6</sub> ·4H <sub>2</sub> O]		

were taken from the *International Tables for X-ray Crystallography*, volume 4 (Ibers and Hamilton 1974).  $R$  and  $R_w$  indices are of the conventional form and are expressed as percentages.

Intensity distributions and systematic absences suggested the space group  $P\bar{3}$ . The structure was solved by direct methods; all three cation positions were revealed by the solution with the best figure of merit. Five of the six anion positions were located on difference-Fourier maps, and the structure was refined to an  $R$  index of 19.5% for an isotropic displacement model. Conversion to anisotropic displacement factors for the cations resulted in convergence at an  $R$  index of 9.2%. The final anion position (OW2) was located on a difference-Fourier map, and the  $R$  index was reduced to 7.9%. Because of the poor quality of the data, attempts to refine anisotropic displacement factors for the anions were unsuccessful. The structure was also refined in the space groups  $P\bar{1}$  and  $P3$  with no improvement to the final  $R$  index or to the structural model. Refinement of the occupancy of the OW2 position suggested that the site is fully occupied. Bond-valence calculations were used to identify the anionic species (Table 3). Positional coordinates and anisotropic and equivalent isotropic displacement factors are given in Table 4. Selected interatomic distances and angles are given in Table 5. The observed and calculated structure factors are presented in Table 6.<sup>1</sup>

Note that needlelike crystals from Granetal may have a different structure than the one described here. The morphology (trigonal prismatic) suggests that the space group is different (the presence of a  $\bar{3}$  axis would result

in a trigonal antiprism). However, attempts to take precession and Gandolfi photographs of these crystals were unsuccessful, in that no reflections were recorded on the films, even after extremely long exposure times.

### DESCRIPTION OF THE STRUCTURE

Coordination polyhedra of cations in the namuwite structure are shown in Figure 2. The S atom, at special position  $2d$  with symmetry 3, is tetrahedrally coordinated by four O atoms. The mean S-O distance (1.45 Å) is similar to that reported for other sulfate minerals. The Zn1 atom, at special position  $2c$  with symmetry 3, is tetrahedrally coordinated by three OH groups and one H<sub>2</sub>O molecule. The bond lengths are statistically identical; the mean value of 1.95 Å is very close to the <sup>65</sup>Zn-O distance (1.97 Å) calculated using ionic radii from Shannon (1976). The OH-Zn1-OH and OH-Zn1-OW angles are 112.9 and 105.7°, respectively. Because of this, the tetrahedra are slightly flattened parallel to  $c$ . The Zn1 site must be completely occupied by Zn<sup>2+</sup> because Cu<sup>2+</sup> does not occur in tetrahedral coordination (Eby and Hawthorne 1993); in addition, Zn<sup>2+</sup> is thought to prefer tetrahedral over octahedral coordination. In sclarite, another mineral with both fourfold- and sixfold-coordinated Zn<sup>2+</sup>, the tetrahedral sites are fully occupied by Zn<sup>2+</sup>, and the deficit in the octahedral sites is made up by Mn<sup>2+</sup> (Grice and Dunn 1989).

The Zn2 atom, at the general position  $6g$ , is coordinated by five OH groups and one O atom (O1) forming a distorted octahedron. Bond lengths from Zn2 to the four equatorial and one apical OH groups show little variation (2.02–2.10 Å and 2.16 Å). However, the distance between the Zn2 cation and the apical O1 atom is much greater (2.43 Å). In general, when the Zn<sup>2+</sup> ion adopts octahedral coordination the result is a regular polyhedron; however, the electron microprobe analyses show that approximately one-third of the Zn2 sites in the structure contain Cu<sup>2+</sup>. It is anticipated that the distortion of the Zn2 octahedron results from the Jahn-Teller effect. The Zn2 octahedra share edges to form CdI<sub>2</sub>-type sheets parallel to (001) (Fig. 3), with one vacancy for every six occupied octahedral sites. Lengths of the five shared octahedral edges vary from 2.685 to 2.972 Å, and the lengths of the seven unshared edges range from 3.002 to 3.100 Å. Because of the distortion introduced by Cu<sup>2+</sup> in the Zn2 sites, the layers are slightly corrugated. The sheets are decorated on both sides by SO<sub>4</sub> and Zn1 $\phi_4$  ( $\phi$  = unspecified anion) tetrahedra (Fig. 4). Each SO<sub>4</sub> tetrahedron shares an apical O1 atom with three octahedra, and each Zn1 $\phi_4$  tetrahedron shares three apical OH2 groups with

<sup>1</sup> A copy of Table 6 may be ordered as Document AM-96-604 from the Business Office, Mineralogical Society of America, 1015 Eighteenth Street NW, Suite 601, Washington, DC 20036, U.S.A. Please remit \$5.00 in advance for the microfiche.

TABLE 3. Bond-valence\* arrangement in namuwite

	Zn1	Zn2	S	Total
O1		0.135(7) <sup>x3</sup> →	1.8(2)	2.2(2)
O2			1.57(9) <sup>x3</sup> ↓	1.57(9)
OH1		0.41(1)		1.16(2)
		0.37(1)		
		0.38(2)		
OH2	0.50(3) <sup>x3</sup> ↓	0.33(2)		1.11(4)
		0.28(2)		
OW1	0.51(6)			0.51(6)
OW2				
Total	2.01(8)	1.91(4)	6.5(3)	

\* Calculated from the curves of Brown (1981).

TABLE 4. Positional coordinates and anisotropic and equivalent isotropic displacement factors

	x	y	z	$U_{eq}$	$U_{11}$	$U_{22}$	$U_{33}$	$U_{23}$	$U_{13}$	$U_{12}$
Zn1	0	0	0.1672(6)	299(14)	138(11)	138(11)	621(36)	0	0	69(6)
Zn2	0.1318(4)	0.7134(4)	0.0006(4)	285(9)	88(10)	78(10)	669(17)	-9(13)	-9(15)	28(9)
S	$\frac{2}{3}$	$\frac{1}{3}$	0.2768(14)	366(31)	271(28)	271(28)	557(76)	0	0	136(14)
O1	$\frac{2}{3}$	$\frac{1}{3}$	0.1429(26)	242(58)						
O2	0.8282(29)	0.5007(29)	0.3239(20)	626(58)						
OH1	-0.3730(19)	0.1083(19)	-0.0861(12)	216(27)						
OH2	-0.1891(22)	0.0609(21)	0.1169(14)	294(34)						
OW1	0	0	0.3519(41)	645(101)						
OW2	0.7173(62)	0.1077(64)	0.6031(36)	1790(172)						

Note:  $U_i$  values were multiplied by  $10^4$ .

three of the six octahedra surrounding the vacant octahedral site. In effect, each vacant site shares two (opposite) faces with  $Zn1\phi_4$  tetrahedra.

The three OH2 molecules forming the base of the  $Zn1\phi_4$  tetrahedron are involved in hydrogen bonding to the basal O1 atoms of the sulfate molecules. The tetrahedral-octahedral-tetrahedral (T-O-T) layers in namuwite are held together by hydrogen bonds to the interstitial OW2 molecules. Details of the hydrogen bonding remain obscure, although the bonding probably involves O2 atoms (2.97 and 3.05 Å from OW2), the OW1 molecule (2.96 Å from OW2), or both. It is possible that the hydrogen bonding involves some disorder, as in the case of synthetic  $Zn_4SO_4OH_2 \cdot 5H_2O$  (Bear et al. 1986).

The  $[Zn(OH)_3(H_2O)]$  tetrahedron present in namuwite also occurs in synthetic  $Zn_5(OH)_8(NO_3)_2 \cdot 2H_2O$  (Stählin and Oswald 1970). Sheets of edge-sharing octahedra with one vacancy for every six filled sites are also apparent in the chalcophanite structure (Post and Appleman 1988). Other minerals with both octahedrally and tetrahedrally coordinated essential Zn include hydrozincite (Ghose 1964), sclarite (Grice and Dunn 1989), and simonkolleite (Allman 1968). In each case the fundamental building unit of the structure is a sheet of octahedra with vacancies that share upper and lower faces with  $Zn\phi_4$  tetrahedra. The ratio of filled to vacant sites is 4:2 for hydrozincite and 4:1 for sclarite and simonkolleite. The layers are held

together by  $CO_3$  groups in hydrozincite,  $Zn\phi_4$  and  $CO_3$  groups in sclarite, and by a layer of  $H_2O$  molecules in simonkolleite.

#### NAMUWITE AND THE SYNTHETIC BASIC ZINC SULFATES

The basic zinc sulfates have the general formula  $Zn_nSO_4OH_2 \cdot mH_2O$ , where  $1 \leq n \leq 7$  and  $0 \leq m \leq 5$ . Namuwite is isomorphous with synthetic  $Zn_4SO_4OH_2 \cdot 4H_2O$ . Both compounds have similar  $a$ -cell dimensions, but the  $c$  parameter in namuwite is somewhat larger. Frias Ferreira da Rocha and Glibert (1972) and Glibert (1977) gave values of 10.274 and 10.32 Å for  $Zn_4SO_4(OH)_2 \cdot 4H_2O$ . The reported values for namuwite are 10.50 (Bevins et al. 1982) and 10.54 Å (this study). The difference could be due to the presence of Cu, which distorts the octahedral sheet. However, Glibert (1977) found that the presence of Cu in synthetic  $(Zn,Cu)_4SO_4OH_2 \cdot 4H_2O$  had little effect on  $c$ ; with 6 at% Cu,  $c = 10.318(6)$  Å, and with 31 at% Cu,  $c = 10.316(7)$  Å.

The structure of  $Zn_4SO_4OH_2 \cdot 4H_2O$  has not been described. However, the structure of  $Zn_4SO_4OH_2 \cdot 5H_2O$  was solved by Bear et al. (1986). Precession photographs

TABLE 5. Interatomic distances (Å) and angles (°) in namuwite

Zn1-OH2 × 3	1.96(2)	O1 <sup>a</sup> -Zn2-OH1 <sup>b</sup>	83.3(6)
Zn1-OW1	1.95(4)	O1 <sup>a</sup> -Zn2-OH1 <sup>c</sup>	94.3(6)
(Zn1-O)	1.95	O1 <sup>a</sup> -Zn2-OH1 <sup>d</sup>	82.6(6)
		O1 <sup>a</sup> -Zn2-OH2 <sup>e</sup>	84.9(6)
Zn2-O1 <sup>a</sup>	2.43(2)	OH1 <sup>b</sup> -Zn2-OH1 <sup>d</sup>	95.1(8)
Zn2-OH1 <sup>b</sup>	2.02(1)	OH1 <sup>b</sup> -Zn2-OH2 <sup>e</sup>	84.7(6)
Zn2-OH1 <sup>c</sup>	2.06(1)	OH1 <sup>b</sup> -Zn2-OH2 <sup>f</sup>	100.3(6)
Zn2-OH1 <sup>d</sup>	2.05(2)	OH1 <sup>c</sup> -Zn2-OH1 <sup>d</sup>	81.7(7)
Zn2-OH2 <sup>e</sup>	2.10(2)	OH1 <sup>c</sup> -Zn2-OH2 <sup>f</sup>	98.1(6)
Zn2-OH2 <sup>f</sup>	2.16(2)	OH1 <sup>c</sup> -Zn2-OH2 <sup>g</sup>	82.2(6)
(Zn2-O)	2.14	OH1 <sup>c</sup> -Zn2-OH2 <sup>h</sup>	99.0(7)
		OH2 <sup>g</sup> -Zn2-OH2 <sup>h</sup>	93.5(9)
S-O1	1.41(3)	(O-Zn2-O)	90.0
S-O2 × 3	1.46(2)		
(S-O)	1.45	O1-S-O2 × 3	109.9(1.0)
		O2-S-O2 <sup>i</sup> × 3	109.0(1.1)
		(O-S-O)	109.5
OH2-Zn1-OH2 <sup>a</sup> × 3	112.9(5)		
OH2-Zn1-OW1 × 3	105.7(5)		
(O-Zn1-O)	109.3		

Note: Equivalent positions:  $a = \frac{1}{3}, \frac{2}{3}, \bar{z}$ ;  $b = \bar{x}, \bar{y} + 1, \bar{z}$ ;  $c = \bar{y}, x - y + 1, z$ ;  $d = y, y - x, \bar{z}$ ;  $e = \bar{y}, x - y, z$ ;  $f = \bar{y} + 1, x - y, z$ .

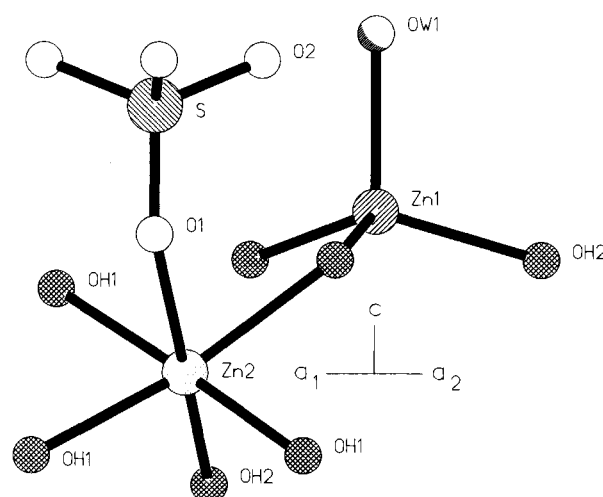


FIGURE 2. Details of the coordination polyhedra in namuwite; S and Zn1 are line shaded, Zn2 is dot shaded, O1 and O2 are open circles, OH1 and OH2 are crosshatched, and OW1 is partially line shaded.

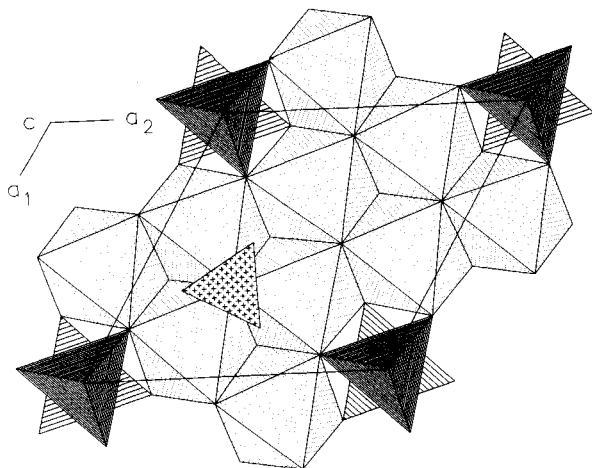


FIGURE 3. The structure of namuwite projected onto (001). The S tetrahedra are shaded with crosses, the Zn1 tetrahedra with parallel lines, and the Zn2 octahedra with dots.

showed that the true symmetry is triclinic, with a pronounced pseudo-hexagonal substructure. Refined cell parameters, from X-ray powder diffraction data, were  $a = 8.354(2)$ ,  $b = 8.350(2)$ ,  $c = 11.001(2)$  Å,  $\alpha = 94.41(2)$ ,  $\beta = 82.95(2)$ ,  $\gamma = 119.93(2)^\circ$ . The structure was refined in the space group  $P\bar{1}$  to an  $R$  index of 3.1%. The results show that the anhydrous components of the structure are similar to those of namuwite, with successive octahedral layers aligned almost vertically, such that the Zn tetrahedra are almost directly above and below one another in adjacent layers. The environments of the interlayer  $H_2O$  positions in the pentahydrate do not correspond to the environment of the OW2 site in namuwite.

Bear et al. (1986) also reported on the structure of  $Zn_4SO_4OH_2 \cdot 3H_2O$ , formed by dehydration of the pentahydrate. Precession photographs showed a doubling of the unit cell; refined cell parameters, from X-ray powder diffraction data, were  $a = 8.367(3)$ ,  $b = 8.393(3)$ ,  $c = 18.569(5)$  Å (i.e.,  $2 \times 9.28$  Å),  $\alpha = 90.29(3)$ ,  $\beta = 89.71(3)$ ,  $\gamma = 120.53(3)^\circ$ . Dehydration was accompanied by twinning, tilting and misorientation of layers and a gradual breakdown in the long-range ordering between layers along  $c$ . The structure was refined in the space group  $I\bar{1}$  to an  $R$  index of 13%. The results show that the centering is due to a displacement of successive octahedral layers by  $\frac{1}{2}[a + b]$ . The environments of the interlayer  $H_2O$  positions in the trihydrate do not correspond to the environment of the OW2 site in namuwite.

Bear et al. (1986) found that unlike the trihydrate,  $Zn_4SO_4OH_2 \cdot 4H_2O$  occupies a very narrow stability region and is extremely difficult to prepare in a pure form. The formation of the tetrahydrate as an intermediate phase (between the penta- and trihydrates) was recorded in a series of precession photographs. These were indexed using an  $I$ -centered triclinic cell with pseudo-hexagonal geometry,  $a \approx b \approx 8.35$  Å,  $c \approx 20.70$  Å (i.e.,  $2 \times 10.35$  Å),  $\alpha \approx \beta \approx 90^\circ$ ,  $\gamma \approx 120^\circ$ . The precession photographs

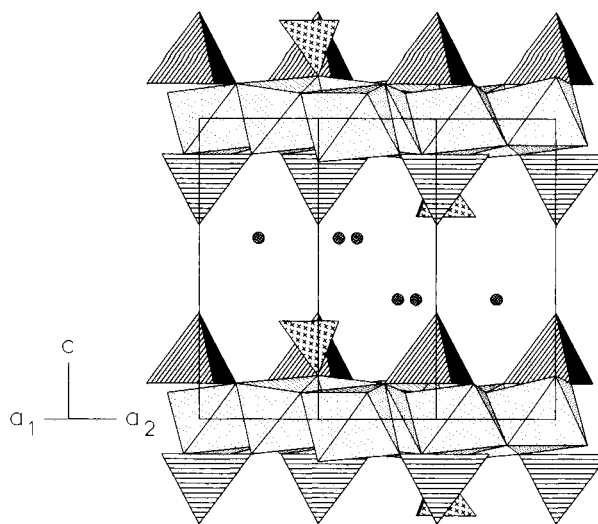


FIGURE 4. The structure of namuwite projected onto (100); shading as in Figure 3. The OW2 atoms are shown as cross-hatched circles.

showed that in the synthetic tetrahydrate, successive octahedral layers are displaced by  $\frac{1}{2}[a + b]$  (Bear et al. 1986). In namuwite, the layers are not displaced. This suggests that the presence of Cu in the octahedral sites prevents displacement of the layers with dehydration, effectively maintaining the anhydrous part of the pentahydrate structure. This may also explain the stability of the namuwite structure relative to that of  $Zn_4SO_4OH_2 \cdot 4H_2O$ .

Is namuwite triclinic? The unconstrained cell dimensions suggest that this may be the case:  $a = 8.331(5)$ ,  $b = 8.334(4)$ ,  $c = 10.543(8)$  Å,  $\alpha = 90.26(5)$ ,  $\beta = 89.79(5)$ ,  $\gamma = 120.00(4)^\circ$ , on the basis of only nine reflections. However, refinement of the namuwite structure in  $P\bar{1}$  resulted in an  $R$  value of 8.1% (cf. 7.9% in  $P\bar{3}$ ) with no significant deviations from the trigonal model. This may indicate that the presence of Cu in the sheets results in higher symmetry, although in most copper oxysalt structures the presence of Cu results in reduced symmetry because of the Jahn-Teller effect (Eby and Hawthorne 1993).

#### THE DEHYDRATION-HYDRATION TRANSITION

Hydration-dehydration transitions in synthetic zinc sulfate compounds were studied by Jacob and Riquier (1969). They synthesized a compound with cell dimensions similar to those published for  $Zn_4SO_4(OH)_6 \cdot 4H_2O$  ( $a = 8.35$  and  $c = 10.326$  Å) but which they described as  $(2.5-3.5)Zn(OH)_2 \cdot ZnSO_4 \cdot (2-2.2)H_2O$ . Irrespective of the hydration state, Jacob and Riquier (1969) found that the  $c$  dimension increased to 10.86 Å in a humid environment at 25 °C. When dried at ambient temperatures, the  $c$  dimension returned to 10.369 Å. This corresponds with the observation by von Hodenberg of a transition in namuwite between 0 and 45 °C in which  $c$  changes from 10.4 to 10.9 Å (W. Krause, personal communication) and with the tetra- to pentahydrate transition studied by Bear

et al. (1986, 1987). Jacob and Riquier (1969) also found that with continued heating the  $c$  parameter fell to 9.27 Å, which is similar to that reported by Bear et al. (1986) for the trihydrate. After prolonged heating at 100–150 °C, this was reduced to 6.98 Å, which is comparable to the thickness of an individual T-O-T layer in namuwite (approximately 7.4 Å).

Bear et al. (1987) found that lower hydrates could be formed from  $Zn_4SO_4(OH)_2 \cdot 5H_2O$  by isothermal heating or by lowering the partial  $H_2O$  pressure. They discovered that the tetrahydrate formed at 32–34 °C, or at  $P_{H_2O}$  of 5–6 mm Hg. The trihydrate formed at 48–50 °C, or at a partial  $H_2O$  pressure of 1.5–5.0 mm Hg. A monohydrate appeared at a partial  $H_2O$  pressure of <1.5 mm Hg. Continued heating resulted in the formation of intergrowth structures at 60–100 °C, a hemihydrate at 100–115 °C, and the anhydrate at 175 °C. The  $c$  parameters for the hemihydrate and the anhydrate were 7.084 and 7.088 Å, respectively. Rehydration to the pentahydrate from the tri- or tetrahydrate was relatively rapid, but from the lower hydrates it took several days.

The presence of Cu in the namuwite structure may serve to lower the temperature of the transition from the tetrahydrate to the pentahydrate. There may also be an upper limit beyond which the dehydration-rehydration transition is irreversible. When the sample used in this study was reexamined several years after the data collection, it was discovered that the originally tabular crystal had split into many very thin, curved plates. Attempts to obtain an X-ray diffraction photograph from the aggregate with a Gandolfi camera were unsuccessful.

#### ACKNOWLEDGMENTS

The author thanks F.C. Hawthorne for suggesting the project and for the use of his equipment. W. Krause supplied the crystals, and M. Raudsepp helped with the electron microprobe analyses. The manuscript was improved by comments from T.S. Ercit and constructive reviews by J.D. Grice and J.E. Post. This work was supported by a research grant from the Natural Sciences and Engineering Research Council of Canada.

#### REFERENCES CITED

- Allman, R. (1968) Refinement of the structure of zinc hydroxide chloride,  $Zn_5(OH)_8Cl_2 \cdot 1H_2O$ . *Zeitschrift für Kristallographie*, 126, 417–426 (in German).
- Bear, I.J., Grey, I.E., Madsen, I.C., Newnham, I.E., and Rogers, L.J. (1986) Structures of the basic zinc sulfates  $3Zn(OH)_2 \cdot ZnSO_4 \cdot mH_2O$ ,  $m = 3$  and 5. *Acta Crystallographica*, B42, 32–39.
- Bear, I.J., Grey, I.E., Newnham, I.E., and Rogers, L.J. (1987) The  $ZnSO_4 \cdot 3Zn(OH)_2 \cdot H_2O$  system: I. Phase formation. *Australian Journal of Chemistry*, 40, 539–556.
- Bertoldi, G., Boscardin, M., and Mattioli, V. (1984) Interesting minerals from Vincenza, Italy. *Lapis*, 9, 18–20 (in German).
- Bevins, R.E., Turgoose, S., and Williams, P.A. (1982) Namuwite,  $(Zn,Cu)_2SO_4(OH)_8 \cdot 4H_2O$ , a new mineral from Wales. *Mineralogical Magazine*, 46, 51–54.
- Brown, I.D. (1981) The bond-valence method: An empirical approach to chemical structure and bonding. In M. O'Keeffe and A. Navrotsky, Eds., *Structure and bonding in crystals*, vol. 2, p. 1–30. Academic, New York.
- Eby, R.K., and Hawthorne, F.C. (1993) Structural relations in copper oxysalt minerals: I. Structural hierarchy. *Acta Crystallographica*, B49, 28–56.
- Frias Ferreira da Rocha, M., and Glibert, J. (1972) Mixed basic sulfates of nickel and zinc. *Bulletin des Societes Chimiques Belges*, 81, 263–277 (in French).
- Ghose, S. (1964) The crystal structure of hydrozincite,  $Zn_5(OH)_8(CO_3)_2$ . *Acta Crystallographica*, 17, 1051–1057.
- Glibert, J. (1977) Basic mixed sulfates of copper and zinc. *Bulletin des Societes Chimiques Belges*, 86, 1–9 (in French).
- Grice, J.D., and Dunn, P.J. (1989) Sclarite, a new mineral from Franklin, New Jersey, with essential octahedrally and tetrahedrally coordinated zinc: Description and structure refinement. *American Mineralogist*, 74, 1355–1359.
- Ibers, J.A., and Hamilton, W.C., Eds. (1974) *International tables for X-ray crystallography*, vol. 4, 366 p. Kynoch, Birmingham, U.K.
- Jacob, M., and Riquier, Y. (1969) Basic sulfates of zinc. *Metallurgie*, 9, 127–139 (in French).
- Livingstone, A., Bridges, T.F., and Bevins, R.E. (1990) Schulerbergite and namuwite from Smallcleugh mine, Nenthead, Cumbria. *Journal of the Russell Society*, 3, 23–24.
- Post, J.E., and Appleman, D.E. (1988) Chalcophanite,  $ZnMn_2O_7 \cdot 3H_2O$ : New crystal-structure determinations. *American Mineralogist*, 73, 1401–1404.
- Rewitzer, C., and Hochleitner, R. (1989) Minerals of the old slags from Lavrion, Greece (Part 2). *Rivista Mineralogica Italiana*, 83–100.
- Schnorrer-Köhler, G. (1986) Mineralogical notes III. *Aufschluss*, 37, 245–254 (in German).
- Schnorrer-Köhler, G., Rewitzer, C., Standfuss, L., and Standfuss, K. (1988) Further new finds in the Laurion antique slags. *Lapis*, 13, 11–14 (in German).
- Shannon, R.D. (1976) Revised effective ionic radii and systematic studies of interatomic distances in halides and chalcogenides. *Acta Crystallographica*, A32, 751–767.
- Stählin, W., and Oswald, H.R. (1970) The crystal structure of zinc hydroxide nitrate,  $Zn_5(OH)_8(NO_3)_2 \cdot 2H_2O$ . *Acta Crystallographica*, B26, 860–863.

MANUSCRIPT RECEIVED DECEMBER 5, 1994

MANUSCRIPT ACCEPTED SEPTEMBER 12, 1995